Scien. Tech. Bull-Chem. Food Sci. Eng., Vol. 17 (XVIII), 2020, 42-48

INDUCTION OF LIQUID CRYSTALLINE PROPERTIES IN PT(II) COORDINATION COMPLEXES BASED ON TERPYRIDINE AND GALLATE LIGANDS

Evelyn POPA[1], Elisabeta I. SZERB[1], Adelina-Antonia ANDELESCU[1*]

[1] "Coriolan Drăgulescu" Institute of Chemistry, Romanian Academy, 24th Mihai Viteazu Bvd.,
Timişoara 300223, Romania
Corresponding author email: andelescu.ade@gmail.com

Abstract: *This paper describes the induction of liquid crystalline properties into a Pt(II) complex based on the tridentate chelating N^N^N ligand 2,6-di(pyridine-2-yl)pyridine-4-(1H)-one, following a strategy reported previously by our group, respectively using a lipophilic gallate unit. Two structurally different Pt(II) species containing one or two gallate units were obtained in the same reaction and were characterized by spectroscopic (FT-IR and ^{1}H NMR) and analytic (elemental analysis) methods. Their liquid crystalline behaviour was assessed by polarized optical microscopy (POM) observations.*

Keywords: Pt(II) metallomesogens, terpyridine Pt(II) coordination complexes, polarized optical microscopy.

INTRODUCTION

Metallomesogens (metal containing liquid crystals) based on *d*-block metal centres are appealing for widespread high-tech, due to the properties arising from both classes: i) metal centres: optical, electronic, magnetic, conductive, dichroic, etc. (Ma *et al.* 2012, Kettle 1996, Darkwah *et al.* 2020, Sanda 2014, Pessoa *et al.* 2009) and ii) liquid crystals: anisotropy of the physical properties, fluidity, stimuli responsiveness, supramolecular complex dynamic and adaptive ordering, etc. (Donnio 2014, Pucci and Donnio 2014). Moreover, their final properties may be improved due to cumulative and/or synergistic effects. Owing to their enhanced properties, metallomesogens are currently under studies for applications in electroluminescent displays (Wu *et al.* 2018a, Rajendiran *et al.* 2020), or as active materials for the fabrication of sensors (Cuerva *et al.* 2016, Cuerva *et al.* 2020, Motoc *et al.* 2019), etc.

A particular interest has been granted to Pt(II) due to the thermodynamic preference of the metal ions to form square planar complexes with strong-field ligands (Williams 2007), property that favours key features regarding absorption, luminescence and other excited state properties. Moreover, it makes it favourite for inducing liquid crystalline properties with respect to other bulkier geometry metals like octahedral Ir(III), Ru(II), tetrahedral Cu(I), Zn(II) etc. (Wu *et al.* 2018b). Therefore, Pt(II) metallomesogens are intensively researched in optoelectronics (Sato et al. 2012, Yang *et al.* 2018, Qian *et al.* 2020). Terpyridines (*tpy*) are commonly being employed as ligands, due to their ability to coordinate a wide variety of metal centres and also because their derivatives show great potential in inducing structural variations, thus obtaining five-, six and nine-coordinate geometries (Kumar *et al.* 2016).

Previously we showed in the case of a Pt(II) complex containing a *tpy* ligand substituted in the apical position with a long alkyl chain (**L-tpyO*R***), that a moderately coordinating gallate unit (**Gal**) can function both as a monodentate ligand, in fulfilling the coordination sphere of Pt(II) or as counterion (Andelescu *et al.* 2020). Furthermore, this strategy allowed us to easily induce liquid crystallinity in the final complex Pt(II) complexes.

Herein we report that by using 2,6-di(pyridine-2-yl)pyridine-4-(1*H*)-one (**L_tpyOH**), the obtainment of two Pt(II) species containing one or two gallate units from a single reaction was achieved (Figure 1).
The two Pt(II) species containing one or two gallate units were characterized by FT-IR and NMR spectroscopies and elemental analysis. Moreover, in case of **Pt_1** and **Pt_2** complexes the liquid crystalline behaviour was assessed by polarized optical microscopy (POM) observations.

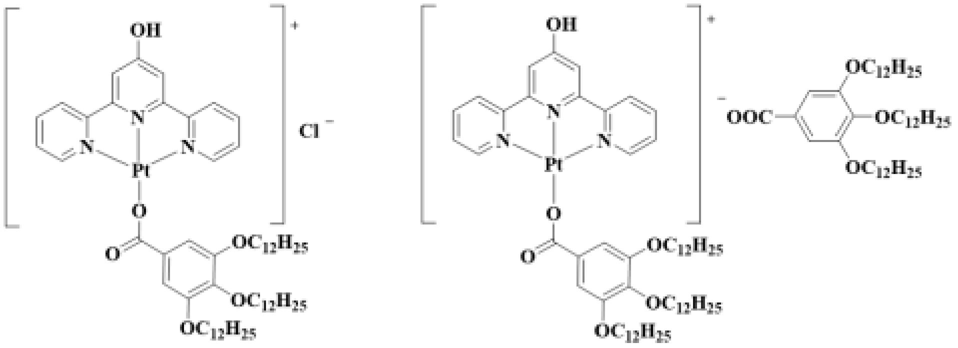

Pt_1 **Pt_2**

Figure 1. The proposed structures of the Pt(II) complexes **Pt_1** and **Pt_2**.

MATERIALS AND METHODS

All commercially available starting materials were used as received without further purification. The ligand **L_tpyOH**, $PtCl_2((CH_3)_2SO)_2$ and the silver complex of 3,4,5-tridodecyloxybenzoic acid (**Ag(Gal)**) were obtained according to reported procedures (Schubert *et al.* 2002, Kukushkin *et al.* 2002, Szerb *et al.* 2013). Infrared spectra (KBr) in the range 4000-400 cm^{-1} were recorded on a Cary 630 FT-IR spectrophotometer. ^{1}H NMR experiments were recorded on a Bruker Fourier 300 MHz spectrometer in DMSO-d$_6$ or $CDCl_3$ using tetramethylsilane (TMS) as internal standard. Elemental analysis C, H and N was performed on a Flash 2000 analyser, by ThermoFisher Scientific, using 1 mg of sample. Two determinations were performed and the average value was used. The optical textures of mesophases were carried out using an Olympus BX53M polarizing microscope (POM) equipped with Linkam hot-stage. Images of the various phases were recorded using an Olympus UC90 camera.

EXPERIMENTAL SECTION

*Synthesis of the **[L_tpyOH(PtCl)]$^+$Cl$^-$** precursor*

[L_tpyOH(PtCl)]$^+$Cl$^-$ *was* synthesized by a slight modification of a method reported in literature for similar derivatives (Annibale *et al.* 1995): a solution of **L_tpyOH** (0.450 g, 1.749 mmol) in 20 mL CH_2Cl_2 was added dropwise over a suspension of $PtCl_2((CH_3)_2SO)_2$ (0.739 g, 1.749 mmol) in 130 mL CH_2Cl_2. The reaction mixture was stirred at room temperature for 4 hours, filtered and washed diethyl ether, yielding a yellow precipitate

[L_tpyOH(PtCl)]$^+$Cl$^-$: yellow precipitate (0.756g, 1.467 mmol, 84%).

FT-IR (KBr, cm^{-1}): 3317 (br, H_2O), 1607-1455(υ(C=C) and υ (C=N)), 442 (υ (Pt–N)).

^{1}H-NMR (300 MHz, DMSO-d$_6$, δ- ppm): 8.90 (d, J = 5.2 Hz, 2H), 8.43 (d, J = 5.8 Hz, 6H), 7.86 (s, 2H), 7.65 (s, 2H).

*Synthesis of **Pt_1** and **Pt_2***

A solution of **Ag(Gal)** (0.456 g, 0.582 mmol) in 20 mL $CHCl_3$ was added dropwise over a suspension of **[L_tpyOH(PtCl)]$^+$Cl** (0.15 g, 0.291 mmol) in 20 mL $CHCl_3$. The reaction mixture was stirred at room temperature for 2 hours, filtered and washed with $CHCl_3$. The mother liquor was taken to dryness. The residue was triturated with hexanes, separated by centrifugation yielding a yellow precipitate (**Pt_2**). The supernatant was evaporated under reduced pressure to give **Pt_1**.

Pt_1: yellow precipitate (0.275 g, 0.195 mmol, 67%)

FT-IR (KBr, cm^{-1}): 2955, 2922, 2852 (C-H stretch), 1635 (ν_{as} (COO$^-$)), 1585-1425 (υ (C=C) and υ (C=N)), 1338 ($\nu_{s,coordinated}$ (COO$^-$)), 445 (υ (Pt–N)).

^{1}H NMR (300 MHz, $CDCl_3$, δ-ppm): 8.49 (d, *J* = 5.72 Hz, 1.52 Hz, 2H), 8.09 (td, *J* = 7.89 Hz, 7.87 Hz, 1.56 Hz, 2H), 7.83 (d, *J* = 8.02 Hz, 2H), 7.42 (overlapped peaks, 4H), 7.35 (s, 2H) 4.05 (overlapped peaks, 6H), 3.69 (broad s, 1H, OH), 2.01 – 1.65 (m, 6H), 1.62-1.14 (overlapped peaks, 54 H), 0.97- 0.73 (m, 9H).

Anal. Calcd. for $C_{59}H_{91}ClN_3O_6Pt{\cdot}H_2O$ (MW = : C, 59.7; H, 7.95; N, 3.54; Found: C, 59.83; H, 7.68; N, 3.31.

Pt_2: orange precipitate (0.02 g, 0.0109 mmol, 3.75 %)
IR (KBr, cm^{-1}): 2953, 2920, 2851 (C-H stretch), 1635 (ν_{as} (COO$^-$)), 1585-1425 (υ (C=C) and υ (C=N)), 1555 ($\nu_{s,ionic}$ (COO$^-$)), 1342 ($\nu_{s,coordinated}$ (COO$^-$)), 445 (υ (Pt–N)).
^{1}H NMR (300 MHz, CDCl$_3$, δ-ppm): 8.48 (dd, *J* = 5.7, 1.5 Hz, 2H), 8.09 (td, *J* = 7.9, 1.6 Hz, 2H), 7.78 (d, *J* = 7.9 Hz, 2H), 7.53 – 7.34 (overlapped peaks, 4H), 7.32 (s, 2H), 7.05 (s, 2H), 4.06 (dt, *J* = 10.5, 6.4 Hz, 12H), 2.88 (broad s, 1H, OH), 1.96 – 1.68 (m, 12H), 1.57 – 1.18 (m, 108H), 0.91 – 0.80 (m, 18H).
Anal. Calcd. for $C_{101}H_{165}N_3O_{11}Pt$ (MW = 1791.21 g/mol): C, 67.68; H, 9.28; N, 2.34; Found: C, 67.99; H, 9.68; N, 2.31.

RESULTS AND DISCUSSIONS

The synthesis of **L_tpyOH** and the silver complex of 3,4,5-tridodecyloxybenzoic acid were carried out as previously reported (Schubert *et al.* 2002, Szerb *et al.* 2013).

Complex **[L_tpyOH(PtCl)]$^+$Cl$^-$** was used as precursor to obtain **Pt_1** and **Pt_2** complexes, by reacting it with 2 equivalents of **Ag(Gal)** (Scheme 1).

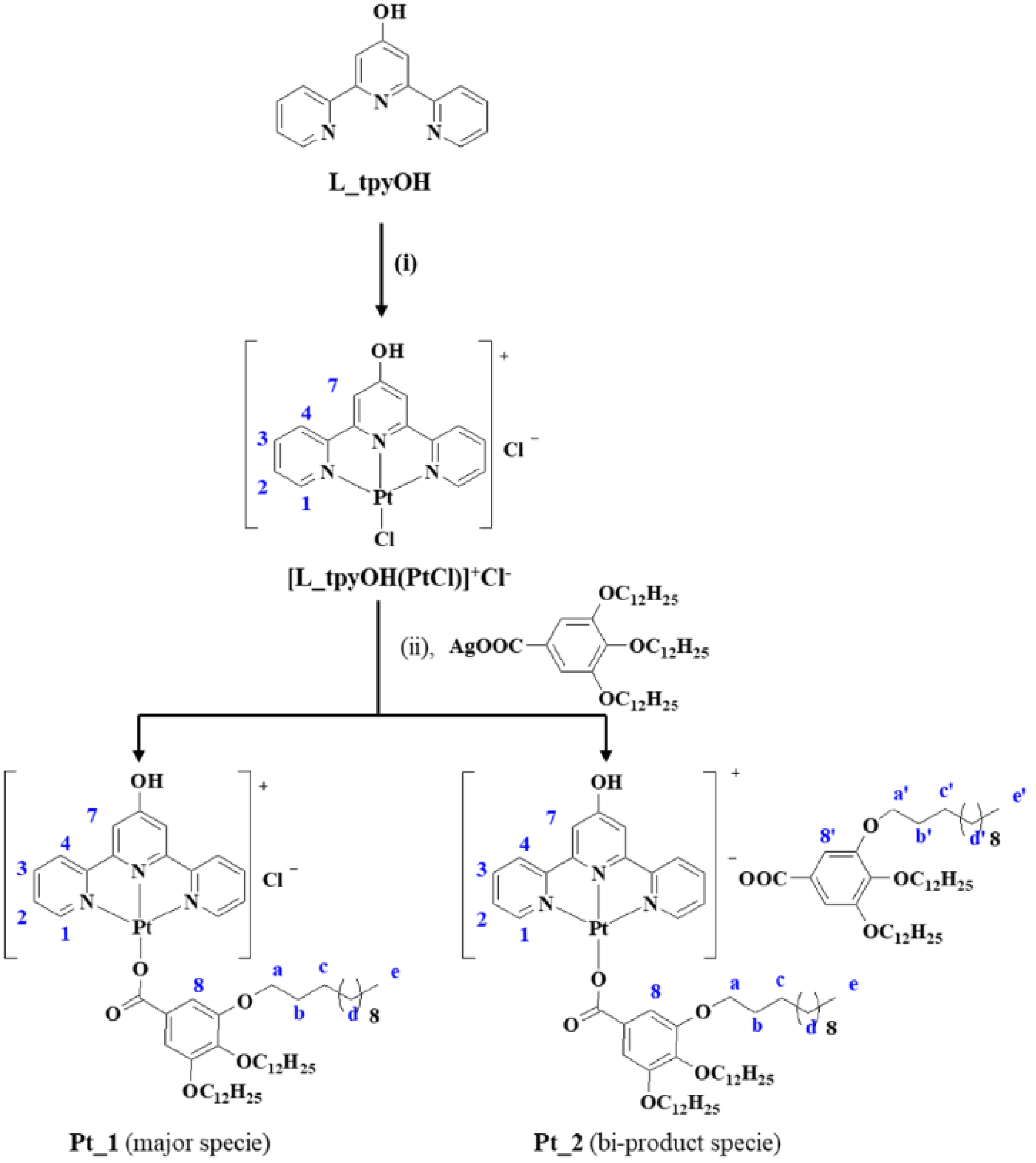

Scheme 1. Reaction pathway of complexes **Pt_1** and **Pt_2** with **L_tpyOH** (atom labelling in blue). Reagents and conditions: (i) $PtCl_2((CH_3)_2SO)_2$, MeOH, r.t., 2 h; (ii) Ag(Gal), $CHCl_3$, r.t, 2 h.

Differently from the previously employed Pt(II) complex containing the ligand **L_tpyO*R*** that when reacted with the silver salt of the gallate **Ag(Gal)** (Andelescu *et al.* 2020) yielded exclusively the complex containing two gallates, herein two species were obtained, probably due to the strong activating group in the apical position. **Pt_1** was obtained as major product and complex **Pt_2** as side product (Scheme 1). All attempts to obtain **Pt_2** as major product complex by changing the reaction conditions (temperature, solvent or reaction time) or reactants ratio failed. Due to the higher solubility of **Pt_2** in hexane, we were able to separate and characterize the compounds. Also, we have investigated the mesomorphic behaviour by POM.

FT-IR spectroscopy.

By comparing the spectra of the free ligand (**L_tpyOH**) with that of **$[L\_tpyOH(PtCl)]^+Cl^-$**, Figure 2, the shifts of the characteristic absorption bands corresponding to $\upsilon_{C=C}$ and $\upsilon_{C=N}$ confirm the successful coordination of Pt(II) centre via the nitrogen atoms of the ligand (Burger *et al.* 2001). Also, in the spectra of the complex, the characteristic absorption band corresponding to υ(Pt–N) is observed at 442 cm^{-1} (Allen and Theophanides 1964).

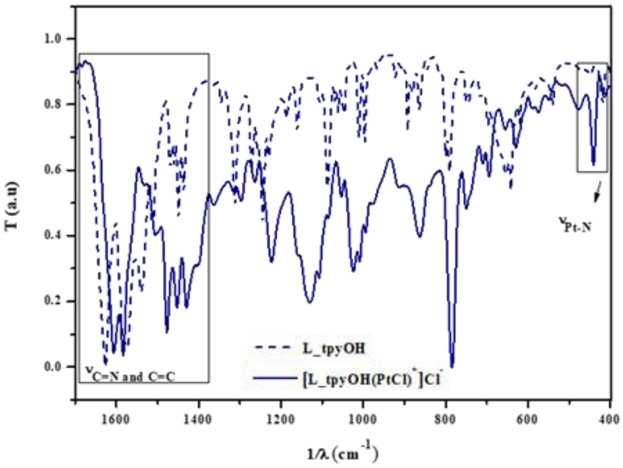

Figure 2. FT-IR spectra of **$[L\_tpyOH(PtCl)]^+Cl^-$** plotted against **L_tpyOH** free ligand.

Moreover, after the exchange of the chlorine ligand and/or counterion with the gallate unit, the dual coordination mode of the gallate group can be noticed by comparing the spectra of the **Pt_1** and **Pt_2** complexes (Figure 3). In particular, the FT-IR spectra of complex **Pt_1** presents the characteristic absorption bands specific of COO^- stretching frequencies: the ν_{as} at 1635 cm^{-1}, and ν_s at 1340 cm^{-1} ($\Delta = 295$ cm^{-1}). Based on literature data (Deacon and Phillips 1980), this value corresponds to a carboxylate unit, which is coordinated to the metal centre. In case of **Pt_2**, two different symmetric COO^- stretching frequencies are observed at: 1555 cm^{-1} (ionic carboxylate) and 1340 (coordinated carboxylate), thus giving a separation (Δ) of 80 and respectively 295 cm^{-1} as seen from Figure 3. The first value corresponds to an ionic carboxylate unit, while the later to a coordinated one.

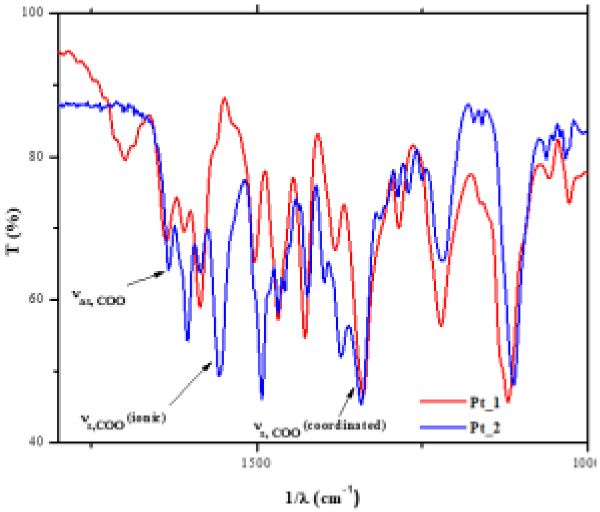

Figure 3. FT-IR spectra of **Pt_1** and **Pt_2**.

^{1}H-NMR spectroscopy

In the ^{1}H-NMR spectra, significant shifts of the aromatic signals associated with the *tpy* protons were observed after complexation. The dual coordination mode of gallate unit is demonstrated also by the ^{1}H-NMR spectroscopy, respectively the aromatic protons belonging to the gallate (Gal) groups have different chemical shifts when coordinated to the metal centre as monodentate ligand (H^8) or when they ensure the neutrality of the complex as negatively charged anion ($H^{8'}$), as shown in Figure 4. In the case of **Pt_1** and **Pt_2**, the aromatic protons belonging to the gallate (Gal) groups have different chemical shifts (Figure 4). In particular, the aromatic proton (H^8) of the gallate unit is observed at 7.35 ppm for complex **Pt_1** and at 7.32 ppm for complex **Pt_2,** showing a coordinated mode, whereas for **Pt_2** the aromatic protons $H^{8'}$, corresponding to the gallate counterion appear at 7.05 ppm.

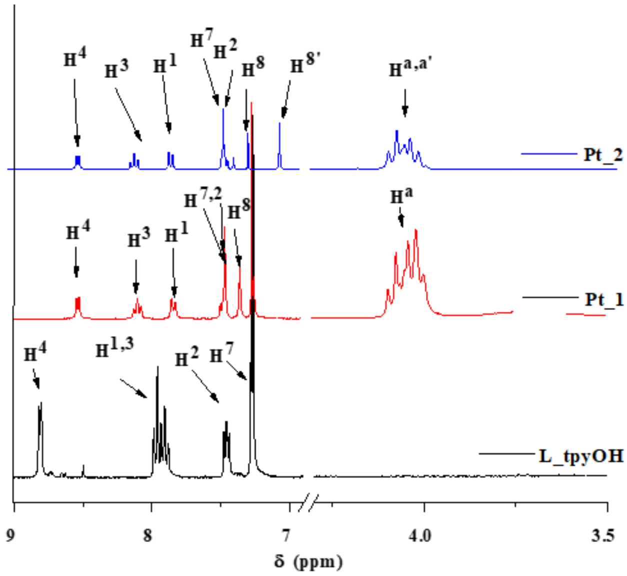

Figure 4. ^{1}H-NMR spectra of ligand **L_tpyOH**, **Pt_1** and **Pt_2** recorded in $CDCl_3$.

Mesomorphic properties

The mesomorphic properties of both **Pt_1** and **Pt_2** complexes was assessed by POM observations. **Pt_1** decomposes before the transition into the isotropic phase, while **Pt_2** has a clearing point at 213°C.

The investigation of the monosubstituted specie **Pt_1** by POM microscopy revealed mesomorphic behaviour on heating. A transition around 83°C from a solid state to a liquid crystalline state is observed, the texture pointing towards a lamellar phase (Figure 5a). The compound decompose before melting around 250°C. Regarding complex **Pt_2**, it exhibit between 70°C and 213°C a columnar phase as identified by the focal-conic texture with homeotropic zones developed on cooling (Figure 5b).

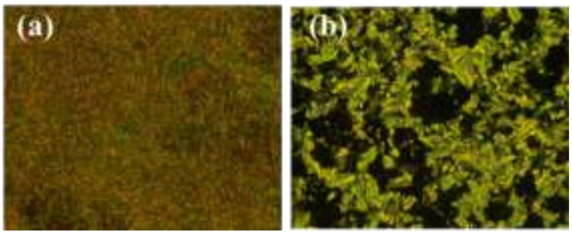

Figure 5. POM micrographs obtained for complex a) **Pt_1** on heating at 200°C and b) **Pt_2** at 175°C on cooling from the isotropic liquid.

CONCLUSIONS

The synthesis of two Pt(II) species, **Pt_1** and **Pt_2**, containing one or two gallate units from a single reaction was achieved using 2,6-di(pyridine-2-yl)pyridine-4-(1*H*)-one as tridentate ligand. The final complexes were characterized through FT-IR and ^{1}H-NMR and elemental analysis.

FT-IR spectroscopy provided information regarding the dual coordination mode of the gallate unit. In case of **Pt_1** the large separation value of the characteristic absorption bands of the carboxylate unit (asymmetrical and symmetrical, $\Delta = 295$ cm^{-1}) suggest that the gallate unit is coordinated to the Pt(II) metal centre, having chlorine as counterion, whereas in case of **Pt_2** two different symmetric COO^- stretching frequencies were observed, indicating that in this case both the displacement of the chlorine counterion and ligand took place.

Furthermore, the chemical shifts of complex **Pt_1** of the aromatic and aliphatic protons were assigned based on ^{1}H NMR acquisitions.

The mesomorphic properties of both **Pt_1** and **Pt_2** complexes were investigated by POM. **Pt_1** developed a texture pointing towards a lamellar phase, while **Pt_2** showed a typical columnar texture.

ACKNOWLEDGEMENTS

Authors acknowledge the Romanian Academy, Program 4. A.A.A. is grateful for an “Ion Heliade Radulescu” mobility scholarship.

REFERENCES

Allen, A.D., Theophanides, T., 1964. Platinum(II) Complexes: Infrared Spectra in the 300–800 cm $^{-1}$ Region. Can. J. Chem. 42(7), 1551–1554. https://doi.org/10.1139/v64-238

Andelescu, A.-A., Heinrich, B., Spirache, M.A., Voirin, E., La Deda, M., Di Maio, G., Szerb, E.I., Donnio, B., Costisor, O., 2020. Playing with Pt^{II} and Zn^{II} Coordination to Obtain Luminescent Metallomesogens. Chem. Eur. J. 26, 4850–4860. https://doi.org/10.1002/chem.202000124

Annibale, G., Brandolisio, M., Pitteri, B., 1995. New routes for the for the synthesis of chloro(diethylenetriamine) platinum(II) chloride and chloro(2,2′ : 6′,2″-terpyridine) platinum(II) chloride dihydrate. Polyhedron 14(3), 451–453. https://doi.org/10.1016/0277-5387(94)00408-7

Burger, K., Wagner, F.E., Vértes, A., Bencze, É., Mink, J., Labádi, I., Nemes-Vetéssy, Z., 2001. Structural Study of Terpyridine and O-Phenanthroline Complexes of Iridium(III). J. Phys. Chem. Solids 62(11), 2059–2068. https://doi.org/10.1016/S0022-3697(01)00075-0

Cuerva, C., Campo, J.A., Cano, M., Lodeiro, C., 2016. Platinum(II) Metallomesogens: New External-Stimuli-Responsive Photoluminescence Materials. Chem. Eur. J. 22(29), 10168–10178. https://doi.org/10.1002/chem.201601115

Cuerva, C., Campo, J.A., Cano, M., Caño-García, M., Otón, J.M., Lodeiro, C. 2020. Aggregation-induced emission enhancement (AIEE)-active Pt(II) metallomesogens as dyes sensitive to Hg^{2+} and dopant agents to develop stimuli-responsive luminescent polymer materials. Dyes Pigm. 175, 108098. https://doi.org/10.1016/j.dyepig.2019.108098

Darkwah, W.K., Sandrine, M.K.C., Adormaa, B.B., Teye, G.K., Puplampu, J.B., 2020. Solar Light Harvest: Modified d-Block Metals. Photocatalysis. Catal. Sci. Technol. 10(16), 5321–5344. https://doi.org/10.1039/C9CY02435B

Deacon, G., Phillips R. J., 1980. Relationships between the Carbon-Oxygen Stretching Frequencies of Carboxylato Complexes and the Type of Carboxylate Coordination. Coord. Chem. Rev. 33(3), 227–250. https://doi.org/10.1016/S0010-8545(00)80455-5

Donnio, B., 2014. Liquid–crystalline metallodendrimers. Inorg. Chim. Acta 409, 53–67. https://doi.org/10.1016/j.ica.2013.07.045

Kettle, S.F.A. Magnetic Properties of Transition Metal Complexes 1996. In Physical Inorganic Chemistry: A Coordination Chemistry Approach, Springer Berlin Heidelberg: Berlin, Heidelberg. https://doi.org/10.1007/978-3-662-25191-1_9

Kukushkin, V.Y., Pombeiro A.J.L., Ferreira C.M.P., Elding L.I., 2002. In Inorganic Syntheses: Dimethylsulfoxide Complexes of Platinum(II): $K[PtCl_3(Me_2SO)]$, cis-$[PtCl_2L(Me_2SO)]$ ($L=Me_2SO$, MeCN), $[PtCl(\mu\text{-}Cl)(Me_2SO)]_2$, and $[Pt(Me_2SO)_4](CF_3SO_3)_2$. John Wiley & Sons, Inc.

Kumar, N.S.S., Shafikov, M.Z., Whitwood, A.C., Donnio, B., Karadakov, P.B., Kozhevnikov, V.N., Bruce, D.W., 2016. Mesomorphism and Photophysics of Some Metallomesogens Based on Hexasubstituted 2,2′:6′, 2″-Terpyridines. Chem. Eur. J. 22(24), 8215–8233. https://doi.org/10.1002/chem.201505072

Ma, D.-L., Ma, V. P.-Y., Chan, D. S.-H., Leung, K.-H., He, H.-Z., Leung, C.-H., 2012. Recent advances in luminescent heavy metal complexes for sensing. Coord. Chem. Rev. 256(23–24), 3087–3113. https://doi.org/10.1016/j.ccr.2012.07.005

Motoc, S., Cretu, C., Costisor, O., Baciu, A., Manea, F., Szerb, E.I., 2019. Cu(I) Coordination Complex Precursor for Randomized CuOx Microarray Loaded on Carbon Nanofiber with Excellent Electrocatalytic Performance for Electrochemical Glucose Detection. Sensors 19(24), 5353. https://doi.org/10.3390/s19245353

Pessoa, J., Correia, I., Gonçalves, G., Tomaz, A. I., 2009. Circular Dichroism in Coordination Compounds. J. Arg. Chem. Soc. 97(1), 151–165. https://doi.org/10.1021/ic50018a026

Pucci, D., Donnio, B., 2014. Metal-Containing Liquid Crystals. In Handbook of Liquid Crystals. 2nd ed., Vol. 5: Non-Conventional Liquid Crystals, Weinheim: Wiley-VCH, pp. 175–241. https://doi.org/10.1002/9783527671403.hlc077

Qian, G., Yang, X., Wang, X., Herod, J.D., Bruce, D.W., Wang, S., Zhu, W., Duan, P., Wang, Y., 2020. Chiral Platinum-Based Metallomesogens with Highly Efficient Circularly Polarized Electroluminescence in Solution-Processed Organic Light-Emitting Diodes. Adv. Opt. Mater. 8(20), 2000775. https://doi.org/10.1002/adom.202000775

Rajendiran, K., Yoganandham, S.T., Arumugam, S., Arumugam, D., Thananjeyan, K., 2020. An Overview of Liquid Crystalline Mesophase Transition and Photophysical Properties of “f Block,” “d Block,” and (SCO)

Spin-Crossover Metallomesogens in the Optoelectronics. J. Mol. Liq. 2020, 114793. https://doi.org/10.1016/j.molliq.2020.114793

Sanda, F., 2015.Transition Metal Containing Polymers. In Encyclopedia of Polymeric Nanomaterials, Springer Berlin Heidelberg: Berlin, Heidelberg, pp. 1–6. https://doi.org/10.1007/978-3-642-36199-9_383-1

Sato, T., Awano, H., Haba, O., Katagiri, H., Pu, Y.-J., Takahashi, T., Yonetake, K., 2012. Synthesis, Characterization, and Polarized Luminescence Properties of Platinum(II) Complexes Having a Rod-like Ligand. Dalton Trans. 41(27), 8379–8389. https://doi.org/10.1039/C2DT30071K

Schubert, U.S., Schmatloch, S., Precup, A., 2002. Access to supramolecular polymers: Large scale synthesis of 4'-chloro-2,2':6',2"-terpyridine and an application to poly(propylene oxide) telechelics. Des. Monomers Polym. 5, 211–221. https://doi.org/10.1163/156855502760157935

Szerb, E.I., Pucci, D., Crispini, A., La Deda, M., 2013. Soft Luminescent Materials Based on Ag(I) Coordination Complexes. Mol. Cryst. Liq. Cryst. 573, 34–45. https://doi.org/10.1080/15421406.2013.763335

Williams, J.A.G., 2007. Photochemistry and Photophysics of Coordination Compounds: Platinum. Top. Curr. Chem. 281, 205-268. https://doi.org/10.1007/128_2007_134

Wu, X., Xie, G., Cabry, C.P., Xu, X. Cowling, S.J., Bruce, D.W., Zhu, W., Baranoff, E., Wang, Y., 2018a. Linearly Polarized Electroluminescence from Ionic Iridium Complex-Based Metallomesogens: The Effect of Aliphatic-Chain on Their Photophysical Properties. J. Mater. Chem. C 6, 3298–3309. https://doi.org/10.1039/C7TC05421A

Wu, X., Zhu, M., Bruce, D.W., Zhu, W., Wang, Y., 2018b. An overview of phosphorescent metallomesogens based on platinum and iridium. J. Mater. Chem. C 6, 9848–9860. https://doi.org/10.1039/C8TC02996B

Yang, X., Wu, X., Zhou, D., Yu, J., Xie, G., Bruce, D.W., Wang, Y., 2018. Platinum-Based Metallomesogens Bearing a Pt(4,6-Dfppy)(Acac) Skeleton: Synthesis, Photophysical Properties and Polarised Phosphorescence Application. Dalton Trans. 47(38), 13368–13377. https://doi.org/10.1039/C8DT03017K